



Outer Membrane Iron Uptake Pathways in the Model Cyanobacterium *Synechocystis* sp. Strain PCC 6803

Guo-Wei Qiu,^a Wen-Jing Lou,^a Chuan-Yu Sun,^a Nina Yang,^b Zheng-Ke Li,^a Ding-Lan Li,^a Sha-Sha Zang,^a Fei-Xue Fu,^b David A. Hutchins,^b Hai-Bo Jiang,^a [®] Bao-Sheng Qiu^a

^aSchool of Life Sciences and Hubei Key Laboratory of Genetic Regulation and Integrative Biology, Central China Normal University, Wuhan, Hubei, People's Republic of China

^bMarine and Environmental Biology, Department of Biological Sciences, University of Southern California, Los Angeles, California, USA

ABSTRACT Cyanobacteria are foundational drivers of global nutrient cycling, with high intracellular iron (Fe) requirements. Fe is found at extremely low concentrations in aquatic systems, however, and the ways in which cyanobacteria take up Fe are largely unknown, especially the initial step in Fe transport across the outer membrane. Here, we identified one TonB protein and four TonB-dependent transporters (TBDTs) of the energy-requiring Fe acquisition system and six porins of the passive diffusion Fe uptake system in the model cyanobacterium Synechocystis sp. strain PCC 6803. The results experimentally demonstrated that TBDTs not only participated in organic ferri-siderophore uptake but also in inorganic free Fe (Fe') acquisition. 55Fe uptake rate measurements showed that a TBDT quadruple mutant acquired Fe at a lower rate than the wild type and lost nearly all ability to take up ferri-siderophores, indicating that TBDTs are critical for siderophore uptake. However, the mutant retained the ability to take up Fe' at 42% of the wild-type Fe' uptake rate, suggesting additional pathways of Fe' acquisition besides TBDTs, likely by porins. Mutations in four of the six porin-encoding genes produced a low-Fe-sensitive phenotype, while a mutation in all six genes was lethal to cell survival. These diverse outer membrane Fe uptake pathways reflect cyanobacterial evolution and adaptation under a range of Fe regimes across aquatic systems.

IMPORTANCE Cyanobacteria are globally important primary producers and contribute about 25% of global CO₂ fixation. Low Fe bioavailability in surface waters is thought to limit the primary productivity in as much as 40% of the global ocean. The Fe acquisition strategies that cyanobacteria have evolved to overcome Fe deficiency remain poorly characterized. We experimentally characterized the key players and the cooperative work mode of two Fe uptake pathways, including an active uptake pathway and a passive diffusion pathway in the model cyanobacterium *Synechocystis* sp. PCC 6803. Our finding proved that cyanobacteria use ferri-siderophore transporters to take up Fe', and they shed light on the adaptive mechanisms of cyanobacteria to cope with widespread Fe deficiency across aquatic environments.

KEYWORDS *Synechocystis*, TonB-dependent pathway, cyanobacteria, iron uptake, porins

cyanobacteria are a diverse group of prokaryotes widely distributed across marine, freshwater, and coastal habitats and are vital players in global marine carbon and nitrogen cycles (1–3). These photosynthetic microorganisms contribute at least 25% of the world's primary productivity (4, 5). Furthermore, diazotrophic cyanobacteria can fix inert dinitrogen (N₂) gas to bioavailable ammonia and contribute up to half of the new nitrogen supporting marine primary production (6, 7).

Received 22 June 2018 Accepted 21 July 2018

Accepted manuscript posted online 3 August 2018

Citation Qiu G-W, Lou W-J, Sun C-Y, Yang N, Li Z-K, Li D-L, Zang S-S, Fu F-X, Hutchins DA, Jiang H-B, Qiu B-S. 2018. Outer membrane iron uptake pathways in the model cyanobacterium *Synechocystis* sp. strain PCC 6803. Appl Environ Microbiol 84:e01512-18. https://doi.org/10.1128/AEM.01512-18.

Editor Shuang-Jiang Liu, Chinese Academy of Sciences

Copyright © 2018 American Society for Microbiology. All Rights Reserved.

Address correspondence to Hai-Bo Jiang, haibojiang@mail.ccnu.edu.cn, or Bao-Sheng Oiu. bsgiu@mail.ccnu.edu.cn.

G.-W.Q. and W.-J.L. contributed equally to this study

It has long been established that iron (Fe) availability is a key control of cyanobacterial community composition and ecological distribution due to the high Fe demand of oxygenic photosynthesis (8) and nitrogen fixation pathways (9-12). In oxygenated marine environments, Fe(II) is oxidized to Fe(III), which tends to rapidly precipitate as low-solubility Fe(III) hydroxides (13, 14). As such, the bioavailable dissolved Fe in aquatic environments exists as either inorganic, free Fe (Fe'), or organically bound Fe and is generally present at low-nanomolar to subnanomolar concentrations (15). The low concentration of Fe plays a crucial role in limiting marine primary productivity (16–19). A number of studies have suggested that dissolved Fe' is the most bioavailable Fe species for cyanobacterial uptake in both marine and freshwater environments (20-24). However, Fe' accounts for less than 1% of the dissolved Fe in surface waters, while much of the dissolved Fe (>99%) is complexed to a variety of organic ligands, including siderophores (24-26). Given the relatively high diversity and low concentration of bioavailable Fe, cyanobacteria have evolved several strategies to adapt to low-Fe environments and meet high intracellular Fe demands.

In Fe-limited environments, many Gram-negative bacteria, including some cyanobacteria, are able to synthesize and secrete strong Fe chelators, such as high-affinity siderophores, to bind Fe and form ferri-siderophore complexes for cellular uptake (27-30). The ferri-siderophore complexes are actively transported across the outer membrane (OM) via the TonB-dependent transport system. The TonB-dependent transport system involves three components, as follows: TonB-dependent transporters (TBDTs) in the OM (28, 29), the ExbB-ExbD complex in the cytoplasmic membrane (CM), and the CM-localized TonB protein with a periplasmic domain. TBDTs bind and transport ferri-siderophores by interacting with the energy transducer TonB, which derives its ion electrochemical potential via ExbB-ExbD complexes (29, 30). In addition to ferri-siderophore complexes, TonB-dependent systems have been reported to transport various substrates, including vitamin B₁₂, phages, colicins, transferrin, citrate, heme, sucrose, etc. (29-31). Some non-siderophore-producing organisms may transport siderophores produced by other organisms (22, 32-34). One example is Synechocystis sp. strain PCC 6803 (Synechocystis 6803). Bioinformatics analysis showed that Synechocystis 6803 does not possess siderophore biosynthesis genes (32), but it has been reported to be capable of acquiring exogenous ferri-siderophores, such as ferrioxamine-B, Feaerobactin (35), and dihydroxamate xenosiderophores secreted by the filamentous cyanobacterium Anabaena variabilis ATCC 29413 (33, 34).

Still, many cyanobacteria do not produce siderophores and/or lack siderophore transport capabilities, suggesting that alternative acquisition strategies are in play (32). One such example is that some cyanobacteria use a reductive uptake strategy and reduce Fe(III) to Fe(II) in the periplasmic space via a CM redox system, followed by transport across the CM facilitated by specific transporters (35-37). Several studies have suggested that some cyanobacteria may be able to combine multiple Fe uptake strategies to increase their access to various Fe substrates (e.g., Fe-organic ligand complexes including siderophores and Fe'), a key capability necessary to thrive in Fe-limited environments (24, 35). For instance, cyanobacteria may be able to acquire Fe via passive uptake across the cell OM (38). Cyanobacteria are Gram-negative bacteria characterized by a semipermeable OM, a peptidoglycan cell wall, and an inner CM (39). The OM contains trimeric β -barrel proteins or porins that facilitate the passive transport of small solutes across the OM and into the cell, such as carbohydrates, amino acids, etc., and may include dissolved unchelated Fe' (40). However, direct evidence of the involvement of OM porins in Fe' uptake is still lacking.

Our recent study found that ExbB-ExbD complexes are required components of Fe' acquisition pathways in Synechocystis 6803, suggesting that TonB-dependent transport systems may be involved in Fe' acquisition and in uptake of ferri-siderophores (41). This study aimed to further elucidate these Fe uptake pathways by focusing on OM transport mechanisms since they remain poorly defined. Specifically, the role of the TonB protein and OM TBDTs in Fe' acquisition have not been identified, and direct evidence for cyanobacterial TBDT involvement in Fe' uptake is still lacking. To dem-

onstrate that ferri-siderophore transport systems can also capture Fe' and to clarify OM Fe uptake pathways in cyanobacteria, we investigated the functions of a putative TonB protein and TBDT proteins in the model cyanobacterium Synechocystis 6803. While our previous study established the energy-providing ExbB-ExbD complexes as important players in the Fe' uptake process (41), our present study provided evidence that TBDTs are directly involved in the uptake of Fe' in Synechocystis 6803, providing new insights on Fe acquisition mechanisms of cyanobacteria and further exploring the roles of OM porins in the Fe' uptake process.

RESULTS

A TonB protein and four TBDTs were identified in Synechocystis 6803. Two putative TonB proteins (SIr1484 and SII0188) have been found in the Synechocystis 6803 database (CyanoBase; http://genome.microbedb.jp/cyanobase/) via BLAST procedure by amino acid sequence similarity with known TonB sequences from other bacteria, such as Escherichia coli and bioinformatic analysis against typical TonB characteristics (42, 43). As shown in Fig. S1 in the supplemental material, both putative TonB proteins have a cytoplasmic transmembrane domain in the N terminus which may serve as a CM anchor, a proline-rich elongated linker that allows them to span the periplasmic space, and antiparallel β -sheets in the C terminus that may interact with the TonB box domain of TBDTs (42, 43).

To investigate whether SIr1484 and SII0188 are TonB proteins, we assessed the protein-protein interaction between them and known ExbD proteins (for details, see Materials and Methods). A yeast two-hybrid assay indicated that Slr1484 had positive interactions with the three known ExbD proteins (SII1405, SII0479, and SIr0678) (Fig. 1A). However, no positive interaction was observed between SII0188 and known ExbD proteins (Fig. S2), suggesting that SII0188 may not be a real TonB. Furthermore, a coimmunoprecipitation (Co-IP) assay was conducted, and the results demonstrated that SIr1484 interacted with the known ExbD protein SIr0678 (Fig. 1C). As with the yeast two-hybrid result, the Co-IP result did not find any interaction between SII0188 and ExbD. Together, these results indicated that SIr1484 is a likely TonB protein, but SII0188 is not.

TonB interacts with OM TBDTs by initiating changes in their protein conformations to allow substrates to pass through. As such, we identified four putative TBDTs, SII1406, SII1206, SII1409, and SIr1490, in Synechocystis 6803 from a BLAST of the cyanobacterial database CyanoBase (http://genome.microbedb.jp/cyanobase/), based on the conserved domains of TBDTs reported in other bacteria. The four putative TBDTs share high amino acid sequence similarities, as shown in Fig. S3. All four putative TBDTs form 22-stranded β -barrels (Fig. S3C), a typical TBDT protein structure, and have a periplasmic exposed TonB box in their N termini (Fig. S3A) (43). Their homologues can be found in almost all sequenced freshwater cyanobacterial species and most coastal species but not in open-ocean species (Table S1), which is consistent with the distribution of associated ExbB-ExbD complexes that work in concert with TBDTs for Fe uptake in cyanobacteria (41). We investigated protein-protein interactions between TonB and the putative TBDTs, and both the yeast two-hybrid assay (Fig. 1B) and glutathione S-transferase (GST) pulldown assay (Fig. 1D) proved that Slr1484 has positive interactions with the four putative TBDTs, further confirming the TonB function of SIr1484 and verifying the putative TBDTs as actual TBDTs in Synechocystis 6803.

Expression of the tonB (slr1484) gene is induced by Fe deficiency, and the slr1484::C.K2 mutant is sensitive to Fe limitation. Similar to known Fe uptake genes, the transcriptional expression of the slr1484 gene is induced by Fe limitation. Quantitative real-time reverse transcription-PCR (qRT-PCR) assays showed that the transcription of slr1484 is upregulated 5-fold following 24 h of growth in Fe-depleted medium (Fig. S4). The upregulation of slr1484 by Fe limitation suggests that the Slr1484 protein may be specifically involved in Fe homeostasis.

To investigate the role of slr1484 in Fe uptake, we knocked out the slr1484 gene by inserting a kanamycin-resistant cassette fragment C.K₂, as previously described (44).

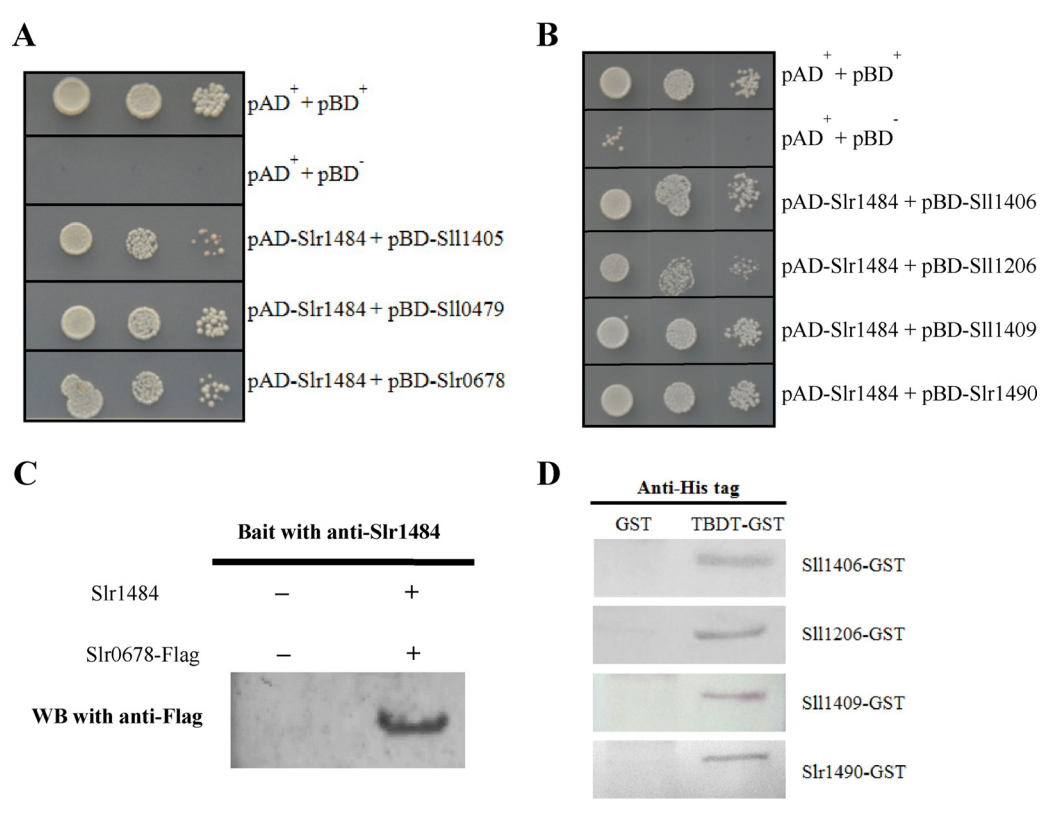


FIG 1 Protein-protein interaction analyses confirmed SIr1484 to be a TonB protein in *Synechocystis* 6803. (A) Yeast two-hybrid assay showing positive interactions between SIr1484 and known ExbD proteins (SII1405, SII0479, and SIr0678). (B) Yeast two-hybrid assay showing positive interactions between SIr1484 and putative TBDTs (SII1406, SII1206, SII1409, and SIr1490). (C) Co-IP assay indicating interaction between SIr1484 and ExbD (SIr0678). Proteins from a *Synechocystis sIr0678-flag* strain were preincubated with anti-SIr1484 antibody and protein A/G plus-agarose. The resulting samples were detected by Western blotting (WB) with anti-FLAG antibody. (D) *In vitro* GST pulldown assay indicating interactions between SIr1484 and putative TBDTs (SII1406, SII1206, SII1409, and SIr1490). GST protein was set as a negative control.

Under Fe-replete conditions, the growth and chlorophyll *a* content of the *slr1484*::C.K₂ mutant were comparable to those of the wild type (Fig. 2A and C). However, when cultivated in Fe-depleted medium, the mutant exhibited an obvious decrease in growth rate compared to the wild type (Fig. 2B). The chlorophyll *a* content of the mutant was also significantly lower than that of the wild-type culture (Fig. 2D). Low-temperature (77 K) fluorescence emission spectral analysis of the Fe depletion-induced marker protein, IsiA, showed that for the wild-type culture, the 682 nm peak in Fe-depleted cultures was significantly induced compared to that of Fe-replete cultures (Fig. 2E and F). Additionally, the induction of IsiA by the *slr1484*::C.K₂ mutant was two times higher than that by the wild type (Fig. 2F), indicating a relatively more pronounced shortage of intracellular Fe in the mutant.

The expression of TBDT-encoding genes is induced by Fe limitation, and the mutation of them leads to an obvious upregulation of known Fe uptake genes. Although the TonB mutant (*slr1484*::C.K₂) exhibited a sensitive phenotype to Fe depletion, we also investigated the function of OM TBDTs, the components that directly capture and transport Fe. We assessed the transcriptional expression of the four TBDT-encoding genes (*sll1406*, *sll1206*, *sll1409*, and *slr1490*) in *Synechocystis* 6803 under different Fe conditions. In wild-type cultures, the expression of TBDT genes was induced by Fe limitation, as determined by qRT-PCR. After 24 h of Fe limitation, the transcriptional levels of *sll1406*, *sll1206*, *sll1409*, and *slr1490* increased 2.1-, 6.4-, 1.6-, and 6.9-fold, respectively (Fig. 3A).

TBDT single mutants were created using genetic transformation by knocking out the four TBDT-encoding genes individually. These single mutants did not exhibit phenotypic differences compared to the wild type when exposed to either Fe-replete or

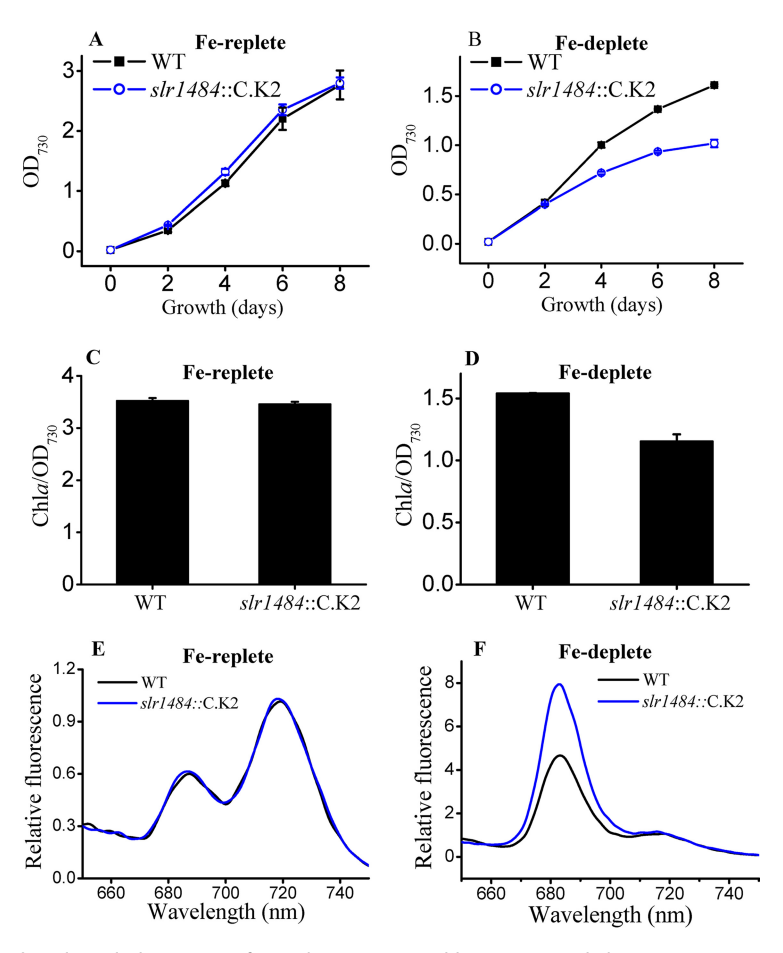


FIG 2 Physiological phenotypes of *Synechocystis* 6803 wild type (WT) and *slr1484*::C.K2 mutant grown with Fe-replete (A, C, and E) and Fe-depleted (B, D, and F) BG-11 medium. (A and B) Growth curves of the cultures determined by optical density at 730 nm (OD $_{730}$). (C and D) Chlorophyll a (Chla) concentration of the cultures. (E and F) Induction level of Fe-induced protein IsiA by 77 K low-temperature fluorescence spectroscopy with excitation wavelength at 430 nm.

Fe-depleted conditions (Fig. S5). Considering that there are four TBDT-encoding genes in the *Synechocystis* 6803 genome and their sequences are highly conserved (Fig. S3), the functions of the four TBDTs are likely redundant, and the remaining TBDTs may compensate for the loss of one of their homologous counterparts. Therefore, we created a quadruple mutant in which all four TBDTs were inactivated by knocking out the TBDT-encoding genes one by one with insertions of different antibiotic resistance genes. In this quadruple mutant, well-known Fe uptake genes (*futA1*, *futA2*, *feoB*, and

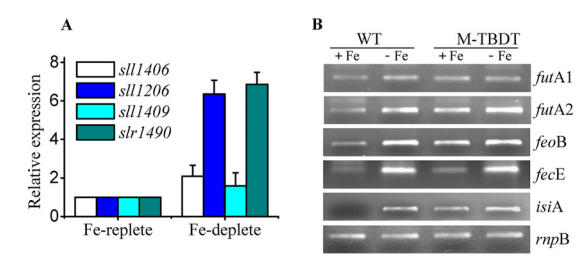


FIG 3 Transcription analysis of *Synechocystis* 6803 Fe uptake-related genes determined by qRT-PCR (A) and RT-PCR analysis (B). (A) Transcript expression levels of putative TBDT-encoding genes from the *Synechocystis* 6803 wild type cultured in Fe-replete and Fe-depleted BG-11 medium for 24 h. (B) Transcript expression levels of known Fe uptake genes in the wild type (WT) and TBDT quadruple mutant (M-TBDT) after incubation under Fe-replete conditions (+Fe) and Fe-depleted conditions (-Fe) for 24 h. The housekeeping gene *rnpB* was used as a reference gene.

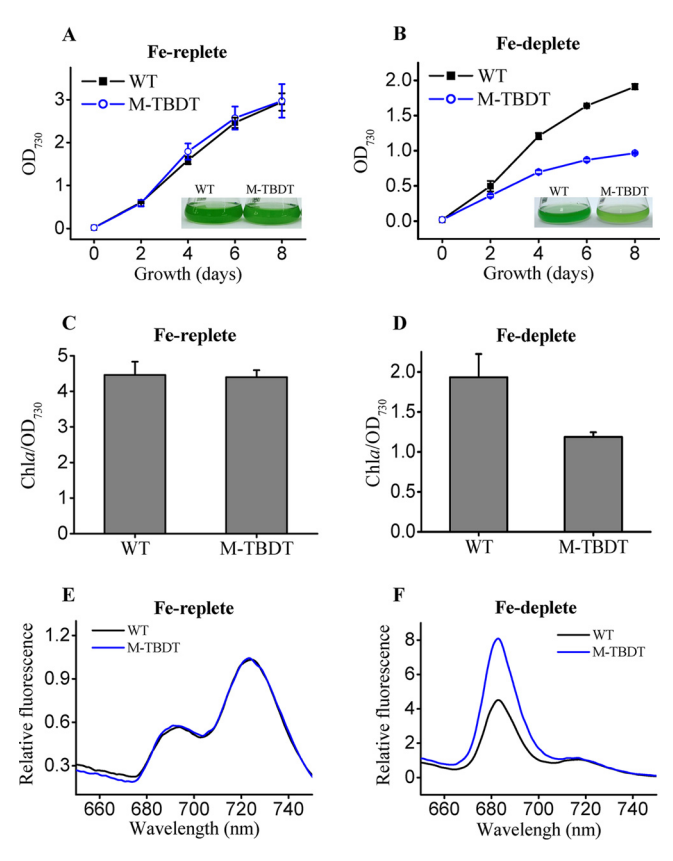


FIG 4 Phenotypic traits of *Synechocystis* 6803 wild type (WT) and TBDT quadruple mutant (M-TBDT) under Fe-replete (A, C, and E) and Fe-depleted (B, D, and F) conditions. The cultures were grown in modified BG-11 medium in which Fe' was the only available Fe resource. (A and B) Growth curves of cultures determined by optical density at 730 nm (OD $_{730}$). The inserted pictures show the cultures after 6 days' growth. (C and D) Chlorophyll a concentration of the cultures. (E and F) Induction level of Fe-induced protein IsiA determined by 77 K low-temperature fluorescence spectroscopy with excitation wavelength at 430 nm.

fecE) and the Fe depletion marker *isiA* were more strongly induced than in the wild type, even under Fe-replete conditions. Some of these genes, such as *isiA* and *futA2*, were even more induced under Fe limitation (Fig. 3B), suggesting that the mutation of all four TBDT-encoding genes resulted in a shortage of intracellular Fe.

TBDT quadruple mutant exhibits a serious disadvantage under Fe'-limiting conditions. To investigate whether cyanobacterial OM TBDTs can take up Fe', we used a modified BG-11 medium with a high concentration of EDTA (10 μ M) and omitted all other organic ligands, such as citrate acid and ammonium ferric citrate (which was replaced with FeCl₃). Because *Synechocystis* 6803 is unable to take up Fe-EDTA (35), the substrate sequestered by the cells was only Fe' in equilibrium with Fe-EDTA. No significant phenotypic differences were observed between the mutant and the wild type under Fe-replete conditions (Fig. 4A, C, and E). After an 8-day incubation period under Fe-depleted conditions, however, the biomass of the TBDT quadruple mutant was less than half of the wild type, and its chlorophyll a content was noticeably lower, at only 61% of that of the wild type (Fig. 4B and D). In addition, the quadruple mutant grown in low-Fe' medium exhibited a higher induction of the Fe-deficient marker protein IsiA, pointing to a greater shortage of intracellular Fe in the mutant (Fig. 4F). All the physiological characteristics described above indicated that the mutation of all four TBDTs resulted in a low-Fe sensitive *Synechocystis* 6803 phenotype.

TBDTs are required for both ferri-siderophores and Fe' uptake in *Synechocystis* **6803**, and the mutation of these proteins could affect intracellular Fe content. To prove that TBDTs of *Synechocystis* 6803 are directly involved in Fe uptake, we compared the intracellular Fe content and short-term radioactive ⁵⁵Fe uptake rates of the TBDT

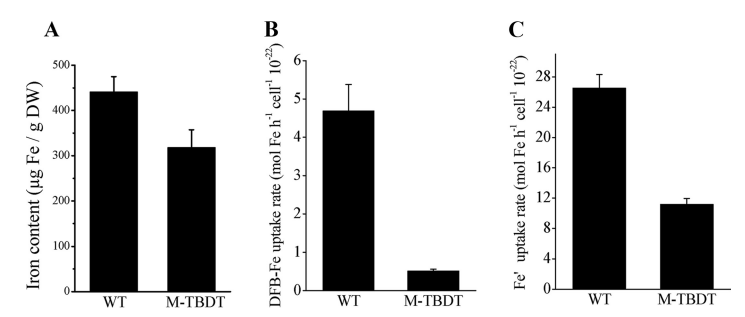


FIG 5 Cellular Fe content (A) and 55 Fe uptake rates (B and C) of *Synechocystis* 6803 WT and TBDT quadruple mutant (M-TBDT). The cells used in these measurements were grown in BG-11 medium to logarithmic phase. The cellular Fe content was normalized to dry weight (DW) cell mass. For measurement of ferri-siderophore uptake rates, 100 nM 55 FeCl $_3$ complexed with 150 nM DFB was added to the cell solutions. For Fe' uptake rate measurements, 280 nM 55 FeCl $_3$ buffered with 16μ M EDTA was added to the cell solutions in which the Fe' concentration is about 0.13 nM, as described in the previous study (41).

quadruple mutant and the wild type grown in standard BG-11 medium. Although the growth rates of the mutant and the wild type were similar under Fe-replete conditions (as shown in Fig. 4A), the TBDT quadruple mutant contained roughly 28% less cellular Fe content than the wild type (Fig. 5A). The lower intracellular Fe content in the mutant is consistent with the higher IsiA induction seen in the mutant (Fig. 3B and 4F).

Short-term 55 Fe uptake assays were conducted with FeCl $_3$ buffered with desferrioxamine-B (DFB) to measure ferri-siderophore uptake and FeCl $_3$ buffered with EDTA to measure Fe' uptake, as previously described by Jiang et al. (41). The results indicated that the TBDTs from *Synechocystis* 6803 were involved in both ferri-siderophore and Fe' uptake processes. Both ferri-siderophore and Fe' uptake rates of the quadruple mutant were lower than those of the wild type. The TBDT quadruple mutant lost nearly all ability to take up DFB-Fe, and the uptake rate was 0.5 ± 0.1 mol Fe \cdot h $^{-1} \cdot$ cell $^{-1} \cdot 10^{-22}$, only 11% of that of the wild type (4.7 \pm 0.7 mol Fe \cdot h $^{-1} \cdot$ cell $^{-1} \cdot 10^{-22}$) (Fig. 5B). However, the Fe' uptake capability in the quadruple mutant was still relatively high (11.2 \pm 0.8 mol Fe \cdot h $^{-1} \cdot$ cell $^{-1} \cdot 10^{-22}$), about 42% of the rate in the wild type (26.5 \pm 1.8 mol Fe \cdot h $^{-1} \cdot$ cell $^{-1} \cdot 10^{-22}$) (Fig. 5C), suggesting the existence of other OM Fe' transporters in *Synechocystis* 6803.

A porin knockdown strain of Synechocystis 6803 resulted in a similar low-Fe sensitive phenotype as the TBDT mutant. It has been speculated that Fe can diffuse across the OM of Gram-negative bacteria through porins. According to bioinformatics analysis, Synechocystis 6803 has six putative porin proteins, SII0772, SII1271, SII1550, SIr0042, SIr1908, and SIr1841. The porin proteins have highly conserved amino acid sequences, and their secondary protein structures form an 18 antiparallel β -barrel with an S-layer domain in the N terminus. Although the porins show a β -barrel structure similar to those of TBDTs, there is no similarity in the amino acid sequences between porins and TBDTs. While TBDTs are mostly found in freshwater and coastal cyanobacterial species (Table S1), putative porin homologues can be found in all sequenced cyanobacterial species (data not shown). We attempted to knock out the six putative porin-encoding genes in Synechocystis 6803, of which only four (sll0772, sll1271, sll1550 and slr0042) were successfully knocked out, and the mutation of five or all six porinencoding genes was lethal to Synechocystis 6803. The porin knockdown strain with inactivation of four of the six porins grew well in Fe-replete medium (Fig. 6A) but grew slower in Fe-depleted medium than the wild type (Fig. 6B). After an 8-day incubation under Fe-depleted conditions, the biomass of the porin knockdown strain was only 68% of the wild type as determined by optical density at 730 nm.

DISCUSSION

It has been widely reported that TonB-dependent transport systems are involved in the transport of organic compounds, especially siderophores for Fe acquisition (30).

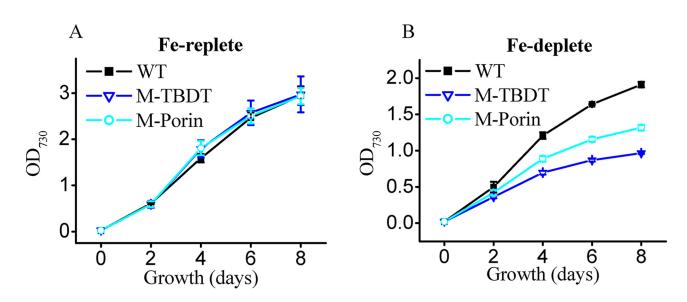


FIG 6 Growth curves of *Synechocystis* 6803 WT, TBDT quadruple mutant (M-TBDT), and porin knockdown strain (M-Porin) under Fe-replete (A) and Fe-depleted (B) conditions.

Using bioinformatic analysis coupled with assays to determine protein-protein interactions, we identified a TonB protein and four TBDT proteins in *Synechocystis* 6803 to clarify their role in OM Fe uptake pathways.

Our study suggested that TBDT-facilitated siderophore uptake pathways are advantageous adaptations in low-Fe environments. Although Fe' has been reported as the most bioavailable of the Fe species for many organisms (20–24), much of the dissolved Fe in aquatic systems is complexed to organic ligands, such as siderophores (e.g., more than 99.9% in marine systems) (45). In our previous study, we found that at Fe-replete concentrations, the Fe' uptake rate of *Synechocystis* 6803 was significantly higher than the ferri-siderophore uptake rate, by 800-fold (41). However, under low-Fe experimental conditions mimicking environmental concentrations, the Fe' uptake rate was only about 5-fold higher than the ferri-siderophore uptake rate (as shown in Fig. 5B and C), indicating that although *Synechocystis* 6803 may prefer Fe', due to the scarcity of bioavailable Fe, siderophore uptake via TonB-dependent systems is an important and supplementary adaptive strategy for Fe acquisition.

It is highly likely that the four TBDTs we reported in Synechocystis 6803 are the only transporters in the OM that bind and transport chelated Fe complexes, because there are only four conserved TBDT-encoding genes and no other homologous genes were found in the Synechocystis 6803 genome. We found no evidence that other OM proteins (e.g., porins) could transport chelated Fe complexes, which are too large for passive transport. The very low DFB-Fe uptake rate of the TBDT quadruple mutant (only 11% of the wild-type uptake rate) further highlighted that these four TBDTs carried out the majority of siderophore uptake and that, without TBDTs, Synechocystis 6803 was nearly incapable of siderophore uptake (Fig. 5B). In our study, the TBDT quadruple mutant was not a lethal mutation, because Fe' was the only Fe source in our modified BG-11 medium and other organic compounds were omitted from the medium except EDTA. Thus, the TBDT quadruple mutant could still acquire Fe' via porins despite losing the ability to take up ferri-siderophore complexes. It can be deduced that the TBDT quadruple mutant could not survive if only given ferri-siderophore as the sole Fe source. Recently, it has been reported that the Synechocystis 6803 wild type could grow with either ferric schizokinen (FeSK) or a siderophore secreted by Anabaena variabilis ATCC 29413 (SAV) as the sole Fe source, but a TonB (SIr1484) mutant and a TBDT (SII1206) mutant could not survive (33, 34). Thus, combining their results and our data, it can be concluded that without TonB-dependent transport system, Synechocystis 6803 is mostly unable to acquire exogenous ferri-siderophores.

Through our TBDT quadruple mutant experiment, we found that TBDTs are not only necessary for ferri-siderophore uptake but are also important in facilitating Fe' uptake, potentially contributing to more than half of the Fe' uptake in *Synechocystis* 6803. We observed a low ⁵⁵Fe uptake rate of the TBDT quadruple mutant measured with ⁵⁵Fe-EDTA and posited that this was due to a loss in the ability to acquire Fe', which could explain why the TBDT quadruple mutant grew worse than the wild type under Fe-limiting conditions when only Fe' was available. When Fe' becomes limiting, the *Synechocystis* 6803 wild type can upregulate its TonB-dependent transport pathway to

facilitate Fe uptake, but the mutant without a complete TonB-dependent pathway can only rely on porin-facilitated passive diffusion which may be insufficient under Fe'limiting conditions.

It has been recently reported that some bacteria are able to use atypical siderophores, such as nicotianamine-like metallophores or even type VI secretion effectors to facilitate Fe acquisition from host cells (46, 47), which raises the possibility that Synechocystis 6803 is also able to secrete unknown Fe chelators; however, the likelihood is very slim. Not only did bioinformatics analysis not find the biosynthesis genes (cntK, cntL, and cntM) of nicotianamine-like metallophores in the Synechocystis 6803 genome, but previous work by Kranzler et al. provided evidence that Synechocystis 6803 does not produce siderophores and cannot scavenge Fe from CAS-Fe(III) (chromeazurol S) during Fe starvation (35). Additionally, our previous study showed that regardless of the total Fe concentration, the Fe uptake rate by Synechocystis 6803 in EDTA-buffered Fe solutions was dependent on the concentration of Fe' (41), making it unlikely for unknown Fe chelators to have a role in Fe acquisition.

Since we did not investigate the Fe' uptake rate mediated by bacterial TBDT, we cannot definitively conclude that only cyanobacterial TBDTs can take up Fe' and that bacterial TBDTs cannot. However, bacterial TonB-dependent transport systems have been intensely studied for more than 30 years, and no report has shown that bacterial TBDTs play a role in Fe' acquisition. Thus, bacterial TBDTs may not be involved in or have a low affinity for Fe', while our results indicate that Synechocystis 6803 TBDTs have a relatively high affinity for Fe'. Autotrophic cyanobacteria have a high Fe demand but inhabit low-Fe environments (32). Although ferri-siderophore uptake could be an important Fe supplement, the dilution of these organic compounds in marine environments may lead to inefficient siderophore acquisition (32). We suggest that the high affinity of TBDTs to Fe' and to siderophores allows cyanobacteria to opportunistically acquire available Fe, regardless of the Fe species. In long-term evolution, the imbalance between high-Fe demand and low-Fe environments may have resulted in cyanobacterial TBDTs developing high Fe' affinity. In our analysis, we noticed that Synechocystis 6803 TBDTs have approximately 90 extra amino acids at the beginning of the N termini compared to their homologues from Escherichia coli, FhuA, IutA, and FepA (Fig. S7). The crystal structure of cyanobacterial TBDTs has to be analyzed to unravel the mechanisms of high affinity for Fe' capture and transport.

The similar growth rates of the TDBT quadruple mutant and the wild type under Fe-replete conditions demonstrated that Fe' acquired by OM porins was likely sufficient to sustain normal metabolic activity. Porin-facilitated passive Fe uptake can be found in all sequenced cyanobacterial species, while TBDT-facilitated active Fe uptake is only found in freshwater and coastal cyanobacterial species (Table S1). In particular, openocean cyanobacteria, such as Prochlorococcus and Synechococcus spp., lack TonBdependent transport systems for Fe uptake and may only rely on porins as the predominant Fe uptake pathway. It has been widely noted that open-ocean cyanobacteria maintain relatively small genomes and have smaller cells than their coastal counterparts that are adapted to steady, albeit low, nutrient concentrations (24, 48). These traits, along with lower Fe requirements, may allow open-ocean cyanobacteria to acquire sufficient Fe solely through porins.

The preferential distribution of TBDT-facilitated Fe uptake in freshwater and coastal waters reflects cyanobacterial adaptations to the variability of Fe species and concentrations across aquatic systems (28, 49). Coastal systems feature higher Fe concentrations and greater Fe variability due to episodic inputs from upwelling and land runoff; open-ocean systems are relatively more constant environments, with lower Fe concentrations (50). Accordingly, coastal cyanobacterial species have higher Fe quotas (51) and active TBDT-facilitated Fe acquisition pathways to accommodate higher Fe requirements than that of open-ocean species. When Fe is readily available, the cells may only need to rely on porins for passive Fe uptake. However, we found that when bioavailable Fe is scarce, the wild-type culture expressed TBDT genes, while the TBDT quadruple mutant was seriously compromised in growth and function. This confirms the impor-

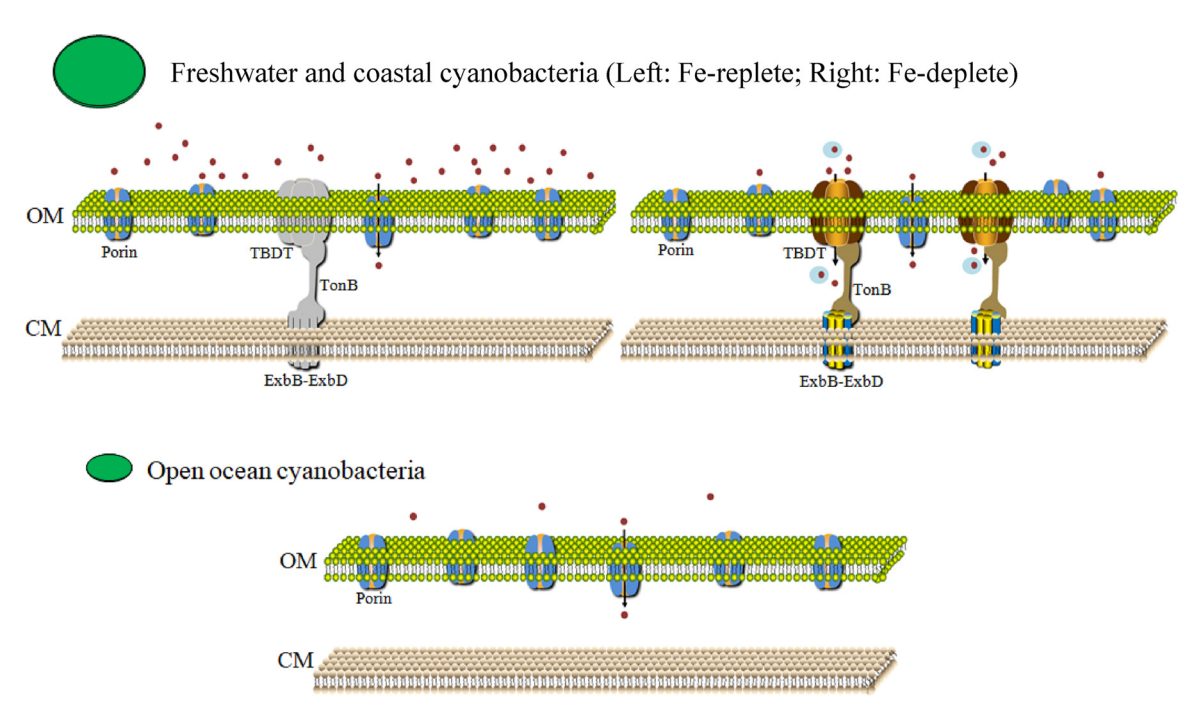


FIG 7 Fe uptake pathways across the outer membrane of two types of cyanobacteria. Freshwater and coastal cyanobacterial species have both porins and OM TonB-dependent transport systems, while open-ocean cyanobacterial species only have porins in the OM. Freshwater and coastal species typically have larger cell sizes and are exposed to higher but more varied Fe concentrations than open-ocean species. When the Fe concentration is high, porins are sufficient to obtain the required Fe for cellular function, and TBDTs are either not expressed or are expressed at low levels. When Fe is limiting, TBDTs are highly induced and actively take up both siderophores and available inorganic Fe'. Open-ocean species are exposed to lower Fe availability but steadier environmental conditions than their freshwater and coastal counterparts, where passive uptake via OM porins can acquire sufficient Fe to meet the cellular Fe requirements of the smaller cells. CM, cytoplasmic membrane; OM, outer membrane.

tance of TonB-dependent systems in Fe uptake under limiting conditions. Based on our findings, we detailed the possible Fe uptake pathways among different cyanobacterial species (Fig. 7).

Despite a growing body of work on Fe acquisition pathways, the initial step in Fe transport across the OM is still poorly described. Our study sheds light on the key players and mechanisms of this critical first step in OM Fe uptake and demonstrates that TonB-dependent transport systems constitute an important and versatile Fe acquisition strategy, providing new insight into the adaptive mechanisms of cyanobacteria to cope with widespread Fe deficiency across aquatic environments.

MATERIALS AND METHODS

Strains, culture conditions, and general methods. A glucose-tolerant strain of *Synechocystis* 6803 was grown in a modified BG-11 medium at 30°C under continuous illumination (30 μ mol photons · m⁻² · s⁻¹). Citric acid was omitted, and ammonium ferric citrate was replaced with Fe-EDTA in the modified medium. The final concentration of EDTA was 10 μ M for both Fe-replete and Fe-depleted medium, and Fe concentrations were 10 μ M and 1 nM for Fe-replete and Fe-depleted medium, respectively. Glassware used for Fe-starved assays was soaked in 6 M HCl for at least 12 h and rinsed six times with Milli-Q water to remove residual Fe. Before cultivation in Fe-depleted medium, exponential cells were harvested by centrifugation and washed two times with Fe-depleted medium to remove extracellular Fe.

Chlorophyll a content was determined spectrophotometrically at OD₆₆₅ in methanol and calculated with the formula chlorophyll a (in milligrams per liter) = $12.6 \times \mathrm{OD}_{665}$. The 77 K chlorophyll fluorescence emission spectra were measured by using an F-4500 fluorescence spectrophotometer (Hitachi, Japan). Cells were grown under Fe-replete or Fe-depleted conditions for 4 days prior and then collected and frozen in liquid nitrogen. The excitation wavelength was set at 430 nm, and the resulting spectra were normalized to the intensity at 720 nm, as previously described (37).

Yeast two-hybrid, coimmunoprecipitation, and GST pulldown assays. Protein-protein interaction between SIr1484 and ExbD proteins or putative TBDTs were detected by a Matchmaker GAL4 two-hybrid system 3 (Clontech, Palo Alto, CA, USA), as previously described (41). The sIr1484 DNA fragment was cloned into a pGADT7 vector, and other genes of this transport system were cloned into a pGBKT7 vector. The resulting plasmids were cotransformed into Saccharomyces cerevisiae AH109, and the resulting

TABLE 1 Strains and plasmids used in this study

Strain or plasmid	Derivation and/or relevant characteristics ^a	Reference or source
Strains		
Synechocystis		
Synechocystis sp. PCC 6803	Wild type	Pasteur culture collection
slr1484::C.K2 mutant	Km ^r , Synechocystis 6803 mutant, result of transformation with pHS3277	This study
M-TBDT mutant	Km ^r Em ^r Sp ^r Gm ^r , <i>Synechocystis</i> 6803 mutant, result of transformation with pHS1569, pHS2749, pHS2751, and pHS2753	This study
M-Porin mutant	Km ^r Em ^r Sp ^r Gm ^r , Synechocystis 6803 mutant, result of transformation with pHS1302, pHS1405, pHS1416, and pHS2635	This study
Yeast	h	
AH109	MAT a trp1-901 leu2-3,112 ura3-52 his3-200 gal4Δ gal80Δ LYS2::GAL1 _{UAS} - GAL1 _{TATA} -HIS3 GAL2 _{UAS} -GAL2 _{TATA} -ADE2 URA3::MEL1 _{UAS} -MEL1 _{TATA} -lacZ	55
AH109(pGADT7-SIr1484/pGKT7-SII1405)	Apr Kmr, AH109 transformed with pHS1776 and pHS3981	This study
AH109(pGADT7-SIr1484/pGKT7-SII0479)	Apr Kmr, AH109 transformed with pHS1776 and pHS3980	This study
AH109(pGADT7-3II1464/pGKT7-3II0479)	Apr Kmr, AH109 transformed with pHS1776 and pHS3979	This study
AH109(pGADT7-SI11464/pGKT7-SI11406)	Apr Kmr, AH109 transformed with pHS1776 and pHS3453	This study
AH109(pGADT7-SIr1464/pGKT7-SII1466)	Apr Kmr, AH109 transformed with pHS1776 and pHS3456	This study
AH109(pGADT7-SIr1484/pGKT7-SII1200) AH109(pGADT7-SIr1484/pGKT7-SII1409)	Apr Kmr, AH109 transformed with pHS1776 and pHS3820	This study
AH109(pGADT7-3II1464/pGKT7-3II1409) AH109(pGADT7-SIr1484/pGKT7-SIr1490)	Apr Kmr, AH109 transformed with pHS1776 and pHS3775	This study
Plasmids	,	
pHS1278	Apr, PCR fragment containing sll1271 cloned into pMD18T	This study
pHS1281	Apr, PCR fragment containing sl11550 cloned into pMD18T	This study
pHS1301	Apr, PCR fragment containing stroots cloned into pMD18T	This study
pHS1302	Apr Kmr, C.K2 cassette from pRL446 inserted into pHS1278 at the Nhel site	This study
pHS1405	Apr Cmr, PCR fragment containing <i>sll0772</i> cloned into pMD18T, and C.CE2	This study
pr131403	inserted in its Hpal site	This study
pHS1416	Apr Spr, Omega cassette from pRL57 inserted into pHS1301 at the Hpal site	This study
pHS1567	Apr, PCR fragment containing <i>sll1406</i> cloned into pMD18T	This study
pHS1569	Apr Kmr, C.K2 cassette from pRL446 inserted into pHS1567 at the Clal site	This study
pHS1776	Apr, PCR fragment containing <i>slr1484</i> cloned into pGADT7 vector	This study
pHS1778	Apr, PCR fragment containing <i>sll0188</i> cloned into pGADT7 vector	This study
pHS1801	Km ^r , PCR fragment containing <i>slr1484</i> cloned into pET28a vector	This study
pHS2107	Gm ^r , a cloning vector with a gentamicin resistance cassette	This study
pHS2635	Apr Gmr, gentamicin resistance cassette from pHS2107 inserted into pHS1281 at the Apal site	This study
pHS2744	Apr, PCR fragment containing sl11409 cloned into pMD18T	This study
pHS2746	Apr, PCR fragment containing <i>sl/1206</i> cloned into pMD18T	This study
pHS2748	Apr, PCR fragment containing <i>str1490</i> cloned into pMD18T	This study
pHS2749	Apr Spr, Omega cassette from pRL57 inserted into pHS2744 at the Ball site	This study
pHS2751	Apr Cmr, C.CE2 cassette from pRL598 inserted into pH52748 at the ball site	This study
pHS2753	Apr Gmr, gentamicin resistance cassette from pHS2107 inserted into pHS2746 at the Clair Site of the Cl	This study This study
pHS3271	Kmr, PCR fragment containing sll1206 cloned into pET41a vector	This study
pHS3272	Km ^r , PCR fragment containing <i>sll1406</i> cloned into pET41a vector	This study
pHS3274	Km ^r , PCR fragment containing <i>sll1490</i> cloned into pET41a vector	This study
pHS3277 pHS3277	Apr Kmr, PCR fragment containing <i>slr1484</i> cloned into pMD18T, and C.K2	This study
	inserted in its Hpal site	
pHS3453	Km ^r , PCR fragment containing <i>sll1406</i> cloned into pGBKT7 vector	This study
pHS3456	Km ^r , PCR fragment containing sll1206 cloned into pGBKT7 vector	This study
pHS3775	Km ^r , PCR fragment containing slr1490 cloned into pGBKT7 vector	This study
pHS3820	Km ^r , PCR fragment containing sll1409 cloned into pGBKT7 vector	This study
pHS3938	Km ^r , PCR fragment containing sll1409 cloned into pET41a vector	This study
pHS3979	Km ^r , PCR fragment containing slr0678 cloned into pGBKT7 vector	This study
pHS3980	Km ^r , PCR fragment containing sll0479 cloned into pGBKT7 vector	This study
pHS3981	Km ^r , PCR fragment containing sll1405 cloned into pGBKT7 vector	This study
pRL446	Km ^r , a cloning vector with a kanamycin resistance marker (C.K2)	56
pRL57	Spr, cloning vector with a spectinomycin resistance cassette omega	57
pRL598	Cm ^r Em ^r , cloning vector with an erythromycin resistance marker (C.CE2)	56
pGADT7	Apr, yeast two-hybrid expression vector with ADH1 promoter and a fusion of GAL4 AD	Clontech

(Continued on next page)

TABLE 1 (Continued)

		Reference or
Strain or plasmid	Derivation and/or relevant characteristics ^a	source
pGBKT7	Km ^r , yeast two-hybrid expression vector a fusion of GAL4 DNA binding domain (DNA-BD)	Clontech
pGADT7-T	Ap ^r , the <i>T-antigen</i> gene cloned into pGADT7	Clontech
pGBKT7-53	Km ^r , the <i>p53</i> gene cloned into pGBKT7	Clontech
pGBKT7-Lam	Km ^r , the <i>lamin C</i> gene cloned into pGBKT7	Clontech

aKmr, kanamycin resistance; Emr, erythromycin resistance; Spr, spectinomycin resistance; Gmr, gentamicin resistance; Apr, ampicillin resistance; Cmr, chloramphenicol

transformants were then grown on synthetic defined (SD)/-Trp-Leu-His-Ade plates for 3 days. The plasmids and strains used in this study are listed in Table 1, in which detailed construction methods are included. The primers used in this study are listed in Table 2.

To run a Co-IP assay assessing the interaction between SIr1484 and SIr0678, a *Synechocystis sIr0678-flag* strain was obtained by a fusion expression of *sIr0678* with a FLAG tag under the control of a *psbAll* promoter, as described previously by Jiang et al. (52). Additionally, an anti-SIr1484 antiserum was obtained as described in our previous studies (41). The *Synechocystis sIr0678-flag* strain grown in BG-11 medium was collected by centrifugation and resuspended in precooling lysis buffer (50 mM Tris-HCl [pH 7.5], 2 mM EDTA, 150 mM NaCl, 0.1% SDS, 1% Triton X-100). After being broken by ultrasonication on ice, the debris and unbroken cells were removed by centrifugation at 11,000 \times *g* and 4°C for 10 min. The supernatant was preincubated overnight with 1 μ g of anti-SIr1484 antibody and 20 μ l of protein A/G Plus-agarose (SC2003; Santa Cruz Biotechnology). After stringent washing with lysis buffer three times, the beads were then harvested and boiled. The processed samples were then analyzed with 12% sodium dodecyl sulfate-polyacrylamide gel (SDS-PAGE) and immunoblotted via Western blotting with anti-FLAG antibody (Sigma-Aldrich). SDS-PAGE and Western blotting were performed using standard methods.

For the GST pulldown assay, His₆-SIr1484 and a GST-tagged TBDT protein were expressed in *Escherichia coli* BL21(DE3) strains via the pET-28a and pET-41a vector, respectively. Cells containing GST or GST fusion protein were broken by a French press at 1,250 lb/in², and debris and unbroken cells were removed by centrifugation. The extracts were purified and immobilized by a GST binding resin (Novagen). After stringent washing in high-ionic-strength phosphate-buffered saline (PBS) buffer (containing 500 mM NaCl) to omit nonspecific binding, the samples were incubated with cell extracts containing a His₆-SIr1484 fusion protein. After an extensive wash step to remove nonspecific binding, the samples were collected and detected by Western blotting with a His₆ tag monoclonal antibody (Invitrogen).

Construction of the mutants of Synechocystis 6803. Synechocystis 6803 mutants were constructed using standard homologous recombination methods. For example, to create the TBDT quadruple mutant, the four TBDT-encoding genes were amplified from the genomic DNA of Synechocystis 6803 and cloned into a pMD18-T vector (TaKaRa). Then, the four genes were inserted with kanamycin, chloramphenicol, spectinomycin, and gentamicin resistance cassettes. The resulting plasmids were transformed into Synechocystis 6803, as previously described (53). Once a single mutant was obtained by homologous recombination, another plasmid was transformed into the mutant. The TBDT quadruple mutant was obtained after four genetic transformations. PCR confirmed that the TBDT quadruple mutant was completely segregated (Fig. S6). The porin and TonB mutants used in this experiment were obtained using similar methods. The primers used are listed in Table 2, and the resulting plasmids and Synechocystis strains are listed in Table 1.

Extraction of RNA and RT-PCR. About 50 ml of cells at exponential-growth phase was harvested by centrifugation and quickly frozen in liquid nitrogen. Total RNA was extracted using a TRIzol reagent kit (Invitrogen), as described previously (44). Before the reverse transcription step, the samples were digested with RNase-free DNase I (TaKaRa) to digest genomic DNA. For RT-PCR, the first-strand cDNA was synthesized using a PrimeScript RT reagent kit (TaKaRa), according to the manufacturer's instructions. The relative concentration of cDNA was evaluated after serial dilutions by PCR using primers rnpB-1 and rnpB-2 and adjusted to the same level according to the brightness of the PCR bands. All the primers used for RT-PCR are listed in Table 2. qRT-PCR was determined with a 7900HT Fast real-time PCR system (Thermo Fisher, USA). The transcript abundance of each gene was calculated relative to the expression of a reference gene *rnpB*.

Determination of cellular Fe contents and Fe uptake rates. Fe content was measured according to methods described by Keren et al. (54) and Nicolaisen et al. (27). Briefly, the exponential cells were collected, washed twice in 10 mM EDTA and Milli-Q water, and then dried and digested to determine elemental content by an atomic absorption spectrometer (catalog no. AA240FS; Varian, Palo Alto, CA, USA), as previously described by Jiang et al. (41).

Fe uptake rates were measured using the radioactive tracer $^{55}\text{FeCl}_3$ (PerkinElmer), as previously described (41, 44). Cells were grown in BG-11 medium until reaching logarithmic phase of growth, and then 1 ml of samples as harvested, washed, and resuspended with fresh Fe-free BG-11 medium to cell density at about 5×10^7 cells \cdot ml $^{-1}$. For Fe' uptake rate measurements, final concentrations of 0.28 μ M $^{55}\text{FeCl}_3$ and 32 μ M EDTA were added to the cell solutions. For DFB-Fe uptake rate measurements, final concentrations of 0.1 μ M $^{55}\text{FeCl}_3$ and 0.15 μ M DFB were added to the cell solutions. Then, samples were incubated under growth conditions, and 200 μ l was collected for measurement after 2, 4, 8, and 24 h of incubation. Finally, the samples were filtered on polycarbonate filters (Poretics) and washed with 2 ml of

TABLE 2 Primers used in this study

Primer	Sequence (5'-3')	Usage ^a
slr1484-1	ATGTCAATCTCTAATTTCTGCCTGACCCAA	a
slr1484-2	TTAGGAATCGGATGACTGCTCCAGATCG	a
sll1406-1	ACGGTGACGGCGTTGATAATAA	a
sll1406-2	TGTCCAGAGGCTAAACTGGTTGCTA	a
sll1206-1 sll1206-2	CCAAACAAAGAAAATTAGGGGAGT TAGGGGGGTGTCCAGTTG	a
sll1409-1	TTGACGGCCTTACATTCTGGTG	a a
sll1409-2	ATCGTAACGAAGTCCTGCAACT	a
slr1490-1	CTCCTGTGTTATCAGATGCCA	a
slr1490-2	TGTCAAAACGCCCTCCCA	a
sll0772-1	ATGGGCTTAATTTGCGGTTTGGC	a
sll0772-2	TTAGAACAAAAGCTGGTGCGTATATGCC	a
sll1271-1	ATGAACTTCACTAAACAGTTTACTTGCC	a
sll1271-2	TTAAAACTTAAAGCTAGTCCTCAAAGCG	a
sll1550-1	GTGAGGACCTCAACCTAACCAATTACCC	a
sll1550-2 slr0042-1	CTAGAAGCTGAAGGTGGTACGAATTACCC ATGAAACAATATCGATTCACTTGGCTCG	a a
slr0042-1	CTAAAATGTGAACGTCGCCCG	a
slr1484Y2H-1	CATATGGAATTTATTGTGGTGGACCCTTCT	b
slr1484Y2H-2	CTCGAGGGAATCGGATGACTGCTCCAGAT	b
sll1405Y2H-1	ACTCCCGGGTTCGGCCCAAACCACGG	b
sll1405Y2H-2	GTTCTGCAGTTAGTTCTTGGGCGTGGCGGCG	b
sll0479Y2H-1	ATACCCGGGCCAATCCGCCGAAGCGC	b
sll0479Y2H-2	CGACTGCAGTCAAGGCATGGCCCCAGCAC	b
slr0678Y2H-1	GTATCCCGGGAGATTTACCCCGAGCT	b
slr0678Y2H-2	GAACTGCAGTTACTGTTGGGGGGCAC	b
sll1406Y2H-1 sll1406Y2H-2	CATATGCCGGTCCAACCCCTGATTTA CTGCAGCTAGAATGTTACGCCAATTTTTCCTAC	b b
sll1206Y2H-1	GAATTCTCTCCGAACCTACAAACGGT	b
sll1206Y2H-2	GTCGACCCACTCAAATGCCAATG	b
sll1409Y2H-1	TCCCCGGGTAAAGATACGCAAACTGGCATTG	b
sll1409Y2H-2	GGTTCTGCAGAAACTGAACCGAAAATGAGCCA	b
slr1490Y2H-1	TCCCCGGGCCGGATCAATTTGACC	b
slr1490Y2H-2	GTTCTGCAGAAATTCCACCGAAATTGTTCCC	b
slr1484Exp-1	CATATGGAATTTATTGTGGTGGACCCTTCT	С
slr1484Exp-2	CTCGAGGGATCGGATGACCGAAAACCC	C C
slr0678flag-1 slr0678flag-2	TGGTGAATCCCATTGAGTTGATGCAAAAGGG TTACTTGTCGTCGTCGTCGTTGTAGTCCTGTTGGGGGGCACTGGG	d d
sll1406Exp-1	CATCTAGACCGGTCCAACCCCTGATTTA	C
sll1406Exp-2	TACTCGAGCTAGAATGTTACGCCAATTTTTCCTAC	c
sll1206Exp-1	CGTCTAGATCTCCGAACCTACAAACGGT	C
sll1206Exp-2	TACTCGAGTTACCACTCAAATGCATAGCCAATG	С
sll1409Exp-1	GCACTAGTAAAGATACGCAAACTGGCATTGA	С
sll1409Exp-2	TACTCGAGTTAAAACTGAACCGAAAATGAGCCA	С
slr1490Exp-1	CCACTAGTCGGATCAATTTGACCGAAGCT	С
slr1490Exp-2	TACTCGAGTTAAAATTCCACCGAAATTGTTCCC	C
rnpB-1	GAGTTGCGGATTCCTGTCA ACTGCTGGTGCGCTCTTAC	e
rnpB-2 slr1484RT-1	CATCAGTCAATTCTCTGCCCAGTCCG	e e
slr1484RT-2	GCAAATTCCGGAGTCTGGAGGGAAG	e
sll1406RT-1	CAACATAGTCCGCATTACGGTGACGG	e
sll1406RT-2	GCACTGGGCACAAAGTAGCTAGCTTCC	e
sll1206RT-1	CGATCGCCTCTCCGAACCTACAAACG	e
sll1206RT-2	GGTCGAATCAGCAATTGTAACCCTTGCG	e
sll1409RT-1	ACGGCCGATCAATCCCAGCTAATACC	е
sll1409RT-2	GGAACAGTACCAGTGCAAGTGAAG	e
slr1490RT-1 slr1490RT-2	GACCGAAGCTGGACTGACC GGGATTGGTCTGTGGCATTAACTTCAACC	e e
slr1295RT-1	ATGGTCCAAAAGTTATCCCGTCGCC	e
slr1295RT-2	TGTTGGCCCCTTCAGACTTAATCCGT	e
slr0513RT-1	ATGACAACTAAGATTTCCCGGCGGAC	e
slr0513RT-2	CCGCCATAACATACCGGCATCTACGG	e
slr1392RT-1	TGGGCAGCCCAATACAGGTAAATCCAC	e
slr1392RT-2	CCTGGAGGAGCAGACTTTGTCG	e
slr1318RT-1	GTTGGATGTTGCCACTCCCATTGCC	e
slr1318RT-2	CAGACGTTTGGCCAATTCTTTGGTGG	e
sll0247RT-1	GTGCAAACCTATGGCAACGACACCG	e
sll0247RT-2	GGTATCCACAATTTGTCCGCCATCGC	e

^aa, used for construction of mutants; b, used for yeast two-hybrid assay; c, used for GST pulldown assay; d, used for coimmunoprecipitation; e, used for RT-PCR.

20 mM *N*-tris(hydroxymethyl)methyl-2-aminoethanesulfonic acid (TES)-KOH (pH 8.0) containing 10 mM EDTA. Then, the samples were placed in 5 ml scintillation fluor (Ultima Gold; Beckman) before counting on a Packard Tri-Carb scintillation counter.

SUPPLEMENTAL MATERIAL

Supplemental material for this article may be found at https://doi.org/10.1128/AEM .01512-18.

SUPPLEMENTAL FILE 1, PDF file, 3.8 MB.

ACKNOWLEDGMENTS

This study was financially supported by the National Natural Science Foundation of China (grants 31770033 and 31470171), the Fundamental Research Funds for the Central Universities (grants CCNU15A02022 and CCNU16KFY03), Shandong Provincial Key Laboratory of Energy Genetics (grant SDKLEG201804), and the National Science Foundation (grants OCE 1657757 and OCE 1538525).

REFERENCES

- Sañudo-Wilhelmy SA, Kustka AB, Gobler CJ, Hutchins DA, Yang M, Lwiza K, Burns J, Capone DG, Raven JA, Carpenter EJ. 2001. Phosphorus limitation of nitrogen fixation by *Trichodesmium* in the central Atlantic Ocean. Nature 411:66–69. https://doi.org/10.1038/35075041.
- Johnson ZI, Zinser ER, Coe A, McNulty NP, Woodward EMS, Chisholm SW. 2006. Niche partitioning among *Prochlorococcus* ecotypes along oceanscale environmental gradients. Science 311:1737–1740. https://doi.org/ 10.1126/science.1118052.
- 3. Zehr JP. 2011. Nitrogen fixation by marine cyanobacteria. Trends Microbiol 19:162–173. https://doi.org/10.1016/j.tim.2010.12.004.
- Flombaum P, Gallegos JL, Gordillo RA, Rincón J, Zabala LL, Jiao N, Karl DM, Li WKW, Lomas MW, Veneziano D, Vera CS, Vrugt JA, Martiny AC. 2013. Present and future global distributions of the marine cyanobacteria *Prochlorococcus* and *Synechococcus*. Proc Nat Acad Sci U S A 110:9824–9829. https://doi.org/10.1073/pnas.1307701110.
- Bullerjahn GS, Post AF. 2014. Physiology and molecular biology of aquatic cyanobacteria. Front Microbiol 5:359. https://doi.org/10.3389/ fmicb.2014.00359.
- Karl D, Letelier R, Tupas L, Dore J, Christian J, Hebel D. 1997. The role of nitrogen fixation in biogeochemical cycling in the subtropical North Pacific Ocean. Nature 388:533–538. https://doi.org/10.1038/41474.
- Karl D, Michaels A, Bergman B, Capone D, Carpenter E, Letelier R, Lipschultz F, Paerl H, Sigman D, Stal L. 2002. Dinitrogen fixation in the world's oceans. Biogeochemistry 57:47–98. https://doi.org/10.1023/ A:1015798105851.
- 8. Raven JA, Evans MCW, Korb RE. 1999. The role of trace metals in photosynthetic electron transport in O_2 -evolving organisms. Photosynth Res 60:111–149. https://doi.org/10.1023/A:1006282714942.
- Moore JK, Doney SC. 2007. Iron availability limits the ocean nitrogen inventory stabilizing feedbacks between marine denitrification and nitrogen fixation. Global Biogeochem Cycles 21:1–12. https://doi.org/10 .1029/2006GB002762.
- Saito MA, Bertrand EM, Dutkiewicz S, Bulygin VV, Moran DM, Monteiro FM, Follows MJ, Valois FW, Waterbury JB. 2011. Iron conservation by reduction of metalloenzyme inventories in the marine diazotroph *Croco-sphaera watsonii*. Proc Natl Acad Sci U S A 108:2184–2189. https://doi.org/10.1073/pnas.1006943108.
- Whittaker S, Bidle KD, Kustka AB, Falkowski PG. 2011. Quantification of nitrogenase in *Trichodesmium* IMS 101: implications for iron limitation of nitrogen fixation in the ocean. Environ Microbiol Rep 3:54–58. https:// doi.org/10.1111/j.1758-2229.2010.00187.x.
- Walworth NG, Fu FX, Webb EA, Saito MA, Dawn M, McIlvin MR, Lee MD, Hutchins DA. 2016. Mechanisms of increased *Trichodesmium* fitness under iron and phosphorus co-limitation in the present and future ocean. Nat Commun 7:12081. https://doi.org/10.1038/ncomms12081.
- Liu X, Millero FJ. 2002. The solubility of iron in seawater. Mar Chem 77:43–54. https://doi.org/10.1016/S0304-4203(01)00074-3.
- Worsfold PJ, Lohan MC, Ussher SJ, Bowie AR. 2014. Determination of dissolved iron in seawater: a historical review. Mar Chem 166:25–35. https://doi.org/10.1016/j.marchem.2014.08.009.
- 15. Morel FMM, Price NM. 2003. The biogeochemical cycles of trace metals

- in the oceans. Science 300:944–947. https://doi.org/10.1126/science .1083545.
- 16. Martin JH, Coale KH, Johnson KS, Fitzwater SE, Gordon RM, Tanner SJ, Hunter CN, Elrod VA, Nowicki JL, Coley TL, Barber RT, Lindley S, Watson AJ, Van Scoy K, Law CS, Liddicoat MI, Ling R, Stanton T, Stockel J, Collins C, Anderson A, Bidigare R, Ondrusek M, Latasa M, Millero FJ, Lee K, Yao W, Zhang JZ, Friederich G, Sakamoto C, Chavez F, Buck K, Kolber Z, Greene R, Falkowski P, Chisholm SW, Hoge F, Swift R, Yungel J, Turner S, Nightingale P, Hatton A, Liss P, Tindale NW. 1994. Testing the iron hypothesis in ecosystems of the equatorial Pacific Ocean. Nature 371: 123–129. https://doi.org/10.1038/371123a0.
- Falkowski PG, Barber RT, Smetacek VV. 1998. Biogeochemical controls and feedbacks on ocean primary production. Science 281:200–207. https://doi.org/10.1126/science.281.5374.200.
- Achilles KM, Church TM, Wilhelm SW, Luther GW, III, Hutchins DA. 2003. Bioavailability of iron to *Trichodesmium* colonies in the western subtropical Atlantic Ocean. Limnol Oceanogr 48:2250–2255. https://doi.org/10.4319/lo.2003.48.6.2250.
- Boyd PW, Jickells T, Law CS, Blain S, Boyle EA, Buesseler KO, Coale KH, Cullen JJ, de Baar HJ, Follows M, Harvey M, Lancelot C, Levasseur M, Owens NP, Pollard R, Rivkin RB, Sarmiento J, Schoemann V, Smetacek V, Takeda S, Tsuda A, Turner S, Watson AJ. 2007. Mesoscale iron enrichment experiments 1993–2005: synthesis and future directions. Science 315:612–617. https://doi.org/10.1126/science.1131669.
- Fujii M, Dang TC, Rose AL, Omura T, Waite TD. 2011. Effect of light on iron uptake by the freshwater cyanobacterium *Microcystis aeruginosa*. Environ Sci Technol 45:1391–1398. https://doi.org/10.1021/es103311h.
- Fujii M, Yeung AC, Waite TD. 2015. Competitive effects of calcium and magnesium ions on the photochemical transformation and associated cellular uptake of iron by the freshwater cyanobacterial phytoplankton *Microcystis aeruginosa*. Environ Sci Technol 49:9133–9142. https://doi .org/10.1021/acs.est.5b01583.
- Kranzler C, Lis H, Finkel OM, Schmetterer G, Shaked Y, Keren N. 2014.
 Coordinated transporter activity shapes high-affinity iron acquisition in cyanobacteria. ISME J 8:409–417. https://doi.org/10.1038/ismej.2013
- Lis H, Shaked Y, Kranzler C, Keren N, Morel FMM. 2014. Iron bioavailability to phytoplankton: an empirical approach. ISME J 9:1003–1013. https://doi.org/10.1038/ismej.2014.199.
- Lis H, Kranzler C, Keren N, Shaked Y. 2015. A comparative study of iron uptake rates and mechanisms amongst marine and fresh water cyanobacteria: prevalence of reductive iron uptake. Life 5:841–860. https://doi.org/10.3390/life5010841.
- Morel FMM, Kustka AB, Shaked Y. 2008. The role of unchelated Fe in the iron nutrition of phytoplankton. Limnol Oceanogr 53:400 – 404. https://doi.org/10.4319/lo.2008.53.1.0400.
- Gledhill M, Buck KN. 2012. The organic complexation of iron in the marine environment: a review. Front Microbiol 3:69. https://doi.org/10 .3389/fmicb.2012.00069.
- 27. Nicolaisen K, Moslavac S, Samborski A, Valdebenito M, Hantke K, Maldener I, Muro-Pastor AM, Flores E, Schleiff E. 2008. Alr0397 is an outer

- membrane transporter for the siderophore schizokinen in *Anabaena* sp. strain PCC. 7120. J Bacteriol 190:7500–7507. https://doi.org/10.1128/JB .01062-08.
- Rudolf M, Kranzler C, Lis H, Margulis K, Stevanovic M, Keren N, Schleiff E. 2015. Multiple modes of iron uptake by the filamentous, siderophoreproducing cyanobacterium, Anabaena sp. PCC 7120. Mol Microbiol 97: 577–588. https://doi.org/10.1111/mmi.13049.
- Miethke M, Marahiel MA. 2007. Siderophore-based iron acquisition and pathogen control. Microb Mol Biol Rev 71:413. https://doi.org/10.1128/ MMBR.00012-07.
- 30. Noinaj N, Guillier M, Barnard TJ, Buchanan SK. 2010. TonB-dependent transporters: regulation, structure, and function. Annu Rev Microbiol 64:43–60. https://doi.org/10.1146/annurev.micro.112408.134247.
- 31. Schauer K, Rodionov DA, de Reuse H. 2008. New substrates for TonB-dependent transport: do we only see the 'tip of the iceberg'? Trends Biochem Sci 33:330–338. https://doi.org/10.1016/j.tibs.2008.04.012.
- 32. Hopkinson BM, Morel FM. 2009. The role of siderophores in iron acquisition by photosynthetic marine microorganisms. Biometals 22:659 669. https://doi.org/10.1007/s10534-009-9235-2.
- 33. Babykin MM, Obando STA, Zinchenko VV. 2018. TonB-dependent utilization of dihydroxamate xenosiderophores in *Synechocystis* sp. PCC 6803. Curr Microbiol 75:117–123. https://doi.org/10.1007/s00284-017-1355-2.
- 34. Obando STA, Babykin MM, Zinchenko VV. 2018. A cluster of five genes essential for the utilization of dihydroxamate xenosiderophores in *Synechocystis* sp. PCC 6803. Curr Microbiol 75:1165–1173. https://doi.org/10.1007/s00284-018-1505-1.
- 35. Kranzler C, Lis H, Shaked Y, Keren N. 2011. The role of reduction in iron uptake processes in a unicellular, planktonic cyanobacterium. Environ Microbiol 13:2990–2999. https://doi.org/10.1111/j.1462-2920.2011.02572.x.
- Katoh H, Hagino N, Grossman AR, Ogawa T. 2001. Genes essential to iron transport in the cyanobacterium *Synechocystis* sp. strain PCC 6803. J Bacteriol 183:2779–2784. https://doi.org/10.1128/JB.183.9.27 79-2784.2001.
- Xu N, Qiu GW, Lou WJ, Li ZK, Jiang HB, Price NM, Qiu BS. 2016. Identification of an iron permease, cFTR1, in cyanobacteria involved in the iron reduction/re-oxidation uptake pathway. Environ Microbiol 18: 5005–5017. https://doi.org/10.1111/1462-2920.13464.
- Jones CM, Niederweis M. 2010. Role of porins in iron uptake by Mycobacterium smegmatis. J Bacteriol 192:6411–6417. https://doi.org/10.1128/JB.00986-10.
- Hoiczyk E, Hansel A. 2000. Cyanobacterial cell walls: news from an unusual prokaryotic envelope. J Bacteriol 182:1191–1199. https://doi .org/10.1128/JB.182.5.1191-1199.2000.
- Nikaido H. 2003. Molecular basis of bacterial outer membrane permeability revisited. Microbiol Mol Biol Rev 67:593–656. https://doi.org/10 .1128/MMBR.67.4.593-656.2003.
- Jiang HB, Lou WJ, Ke WT, Song WY, Price NM, Qiu BS. 2015. New insights into iron acquisition by cyanobacteria: an essential role for ExbB-ExbD complex in inorganic iron uptake. ISME J 9:297–309. https://doi.org/10 .1038/ismej.2014.123.
- 42. Chu BC, Peacock RS, Vogel HJ. 2007. Bioinformatic analysis of the TonB protein family. Biometals 20:467–483. https://doi.org/10.1007/s10534 -006-9049-4.

- Mirus O, Strauss S, Nicolaisen K, von Haeseler A, Schleiff E. 2009. TonBdependent transporters and their occurrence in cyanobacteria. BMC Biol 7:68. https://doi.org/10.1186/1741-7007-7-68.
- Jiang HB, Lou WJ, Du HY, Price NM, Qiu BS. 2012. Sll1263, a unique cation diffusion facilitator protein that promotes iron uptake in the cyanobacterium *Synechocystis* sp. strain PCC 6803. Plant Cell Physiol 53: 1404–1417. https://doi.org/10.1093/pcp/pcs086.
- Rue EL, Bruland KW. 1995. Complexation of iron(III) by natural organic ligands in the Central North Pacific as determined by a new ligand equilibration/adsorptive stripping voltametric method. Mar Chem 50: 117–138. https://doi.org/10.1016/0304-4203(95)00031-L.
- Ghssein G, Brutesco C, Ouerdane L, Fojcik C, Izaute A, Wang S, Hajjar C, Lobinski R, Lemaire D, Richaud P, Voulhoux R, Espaillat A, Cava F, Pignol D, Borezée-Durant E, Arnoux P. 2016. Biosynthesis of a broad-spectrum nicotianamine-like metallophore in Staphylococcus aureus. Science 352: 1105–1109. https://doi.org/10.1126/science.aaf1018.
- 47. Lin J, Zhang W, Cheng J, Yang X, Zhu K, Wang Y, Wei G, Qian PY, Luo ZQ, Shen X. 2017. A Pseudomonas T6SS effector recruits PQS-containing outer membrane vesicles for iron acquisition. Nat Commun 8:14888. https://doi.org/10.1038/ncomms14888.
- Yelton AP, Acinas SG, Sunagawa S, Bork P, Pedrós-Alió C, Chisholm SW.
 2016. Global genetic capacity for mixotrophy in marine picocyanobacteria. ISME J 10:2946–2957. https://doi.org/10.1038/ismej.2016.64.
- Morrissey J, Bowler C. 2012. Iron utilization in marine cyanobacteria and eukaryotic algae. Front Microbiol 3:43. https://doi.org/10.3389/fmicb .2012.00043.
- Bruland KW, Donat JR, Hutchins DA. 1991. Interactive influences of bioactive trace metals on biological production in oceanic waters. Limnol Oceanogr 36:1555–1577. https://doi.org/10.4319/lo.1991.36.8.1555.
- Sunda WG, Swift DG, Huntsman SA. 1991. Low iron requirement for growth in oceanic phytoplankton. Nature 351:55–57. https://doi.org/10 .1038/351055a0.
- Jiang HB, Song WY, Cheng HM, Qiu BS. 2015. The hypothetical protein Ycf46 is involved in regulation of CO₂ utilization in the cyanobacterium Synechocystis sp. PCC 6803. Planta 241:145–155. https://doi.org/10.1007/ s00425-014-2169-0.
- 53. Jiang HB, Cheng HM, Gao KS, Qiu BS. 2013. Inactivation of Ca^{2+}/H^+ exchanger in *Synechocystis* sp. strain PCC 6803 promotes cyanobacterial calcification by upregulating CO_2 -concentrating mechanisms. Appl Environ Microbiol 79:4048 4055. https://doi.org/10.1128/AEM.00681-13.
- 54. Keren N, Aurora R, Pakrasi HB. 2004. Critical roles of bacterioferritins in iron storage and proliferation of cyanobacteria. Plant Physiol 135: 1666–1673. https://doi.org/10.1104/pp.104.042770.
- 55. James P, Halladay J, Craig EA. 1996. Genomic libraries and a host strain designed for highly efficient two-hybrid selection in yeast. Genetics 144:1425–1436.
- Elhai J, Wolk CP. 1988. A versatile class of positive-selection vectors based on the nonviability of palindrome-containing plasmids that allows cloning into long polylinkers. Gene 68:119–138. https://doi.org/10.1016/ 0378-1119(88)90605-1.
- 57. Black TA, Cai Y, Wolk CP. 1993. Spatial expression and autoregulation of *hetR*, a gene involved in the control of heterocyst development in Anabaena. Mol Microbiol 9:77–84. https://doi.org/10.1111/j.1365-2958 .1993.tb01670.x.